

A NUMERICAL INVESTIGATION OF INERTIA FLOWS OF REGULARIZED HERSCHEL-BULKLEY FLUID VIA A MULTI-FIELD STABILIZED METHOD

Cleiton Fonseca, cfonseca@mecanica.ufrgs.br

Fernando Borges, fborges@mecanica.ufrgs.br

Sergio Frey, frey@mecanica.ufrgs.br

Laboratory of Applied and Computational Fluid Mechanics (LAMAC)
Mechanical Engineering Department, UFRGS
Rua Sarmiento Leite, 425 – 90059-170 –Porto Alegre, RS, Brazil.

Abstract. *The majority of real liquids found in nature behave like non-Newtonian fluids, a fact that makes their study of significant importance to various areas of engineering. Among these non-linear liquids, some of them may exhibit little or no deformation up to a certain stress level - called the yield stress of the material. The present work aimed to simulate viscoplastic fluid flows through an one-to-four abrupt planar expansion via a finite element methodology. This work has employed a multi-field mechanical model based on equations of mass conservation and momentum balance coupled with the Herschel-Bulkley viscoplastic model, regularized by the Papanastasiou equation. This model has been approximated by a multi-field Galerkin-least-squares-type method. This stabilized method overcomes the compatibility conditions involving the finite element sub-spaces for stress-velocity and pressure-velocity - the latter known as Babuška-Brezzi condition, allowing in this way the use of equal-order finite element interpolations. In order to investigate the influence of how the yield stress, the power-law coefficient, the flow-rate and inertia affect the viscoplastic fluid dynamics, the Herschel-Bulkley number has been varied from 0.1 to 100, the power-law coefficient from 0.37 to 1.5, the dimension inlet velocity from 2 to 20 and Reynolds number from 1 to 10. All results have proved to be in accordance with the viscoplastic literature.*

Keywords: *Viscoplastic fluids; Herschel-Bulkley model; Papanastasiou regularization, multi-field stabilized formulations; Galerkin least-squares method.*

1. INTRODUCTION

Many industrial processes of significant relevance for engineering involve flows of liquids which viscosities change with the shear rate - the so-called shear-thinning or shear-thickening non-Newtonian fluids (Bird *et al.*, 1987). In addition, some of them may show a more complex behavior, presenting a yield stress limit which is responsible for the formation of two distinct material regions (see, for instance, Barnes (1999) and references therein). In one of them, known as the unyielded region, the shear stress level applied to the material lies below its yield limit and consequently no-deformation occurs with the material moving as a rigid body. In the other one, called the yielded region, the shear stress level lies beyond the yield limit, forcing the material to flow. Initially called Bingham plastics, nowadays this class of liquids is known as a viscoplastic material. Paint, slurries, pastes, and food products such as margarine, mayonnaise and ketchup, are good examples of this material.

In the last decades, some constitutive hypotheses have been introduced in a tentative to describe the stress-deformation behavior of those materials and different yield criteria presented. Among them, the Bingham plastic and the Herschel-Bulkley fluid are firstly considered (Astarita and Marrucci, 1974). In this article, the latter has been studied, a classical three-parameter viscoplastic model which has been already applied to a wide range of real liquids. Recently, Papanastasiou (1987) introduced a new constitutive equation for yielding materials that concerns the regularization of classical viscoplastic models. This equation presents two important advantages in relation to the classical viscoplastic models. First, it introduces a numerical parameter to control the exponential growth of the shear stress in material regions subjected to very high shear rate values, and it is also valid for both yielded and unyielded zones of the material.

Fluid problems involving the flow of non-Newtonian liquids through sudden expansions has been studied for many researchers, due to their industrial relevance (see, for instance, Alexandrou, *et al.*, (2001) and Pascal *et al.*, (2001)). In particular, for yielding fluids, the investigation of viscoplastic phenomena along those flows brings a broad insight in the material rheology. In this work, inertialess flows of Herschel-Bulkley fluids, regularized by Papanastasiou (1987) strategy, through an one-to-four planar sudden expansion have been numerically simulated. The employed mechanical model considered a multi-field formulation built with continuity and momentum equations coupled with the regularized Herschel-Bulkley constitutive equation. This model has been approximated via a stabilized multi-field finite element method, based on the Galerkin least-squares methodology (Franca and Frey, 1992), with extra-stress, velocity and pressure fields as primal variables. The method has no need to satisfy the inf-sup conditions arisen from finite element sub-spaces for extra-stress, velocity and pressure. Besides, due to the adding of least-squares mesh-dependent terms of residual of Euler-Lagrangian equations, the method eliminates spurious oscillations, inherent to central difference

schemes (Brooks and Hughes, 1982), in high advective-dominated flows. In order to investigate the effect of yield stress, shear-thinning and shear-thickening, flow-rate and inertia on the morphology of material yield surfaces, this article undertook a sensibility analysis ranging the Herschel-Bulkley number from 0.1 up to 100, power-law index from 0.37 to 1.5, dimensionless inlet velocity from 2 to 20 and Reynolds number from 1 to 10. All numerical results have confirmed the stability features of the employed stabilized method and were in agreement with related literature.

2. MECHANICAL MODELING

According to mass conservation and momentum balance principles (Astarita and Marrucci, 1974), incompressible fluid flows may be modeled by the following system of equations,

$$\begin{aligned} \operatorname{div} \mathbf{u} &= 0 \\ \rho D_t \mathbf{u} &= \operatorname{div} \mathbf{T} + \rho \mathbf{g} \end{aligned} \quad (1)$$

where \mathbf{u} is the fluid velocity, ρ its density, \mathbf{T} the stress tensor and \mathbf{g} the gravitational acceleration.

2.1. Viscoplastic constitutive equation

One of the most used viscosity functions employed to fit viscoplastic material data is the Herschel-Bulkley equation. It is a three-rheological-parameter model employing the material yield stress, τ_0 , the consistency index, K , and the power-law coefficient, n . The shear stress field predicted by the classical Herschel-Bulkley model may be expressed as

$$\begin{aligned} \tau &= \tau_0 + K \dot{\gamma}^n & \text{if } \tau > \tau_0 \\ \dot{\gamma} &= 0 & \text{if } \tau < \tau_0 \end{aligned} \quad (2)$$

where τ is the magnitude of the shear stress tensor, $\boldsymbol{\tau}$, and $\dot{\gamma}$ the magnitude of the strain rate tensor, $\mathbf{D} = 1/2(\nabla(\mathbf{u}) + \nabla(\mathbf{u})^T)$,

$$\tau = (1/2 \operatorname{tr} \boldsymbol{\tau}^2)^{1/2} \quad (3)$$

and

$$\dot{\gamma} = (2 \operatorname{tr} \mathbf{D}^2)^{1/2} \quad (4)$$

Eq. (2) characterizes two distinct material regions, namely a unyielded zone in which the applied shear stress is less than the material yielded limit, $\tau < \tau_0$ – with the material behaving as rigid body – and an yielded one where $\tau > \tau_0$ – with the material flowing as a shear-thinning or shear-thickening fluid. Between these two zones, lies a transition surface, called yield surface, for which $\tau = \tau_0$.

The classical Herschel-Bulkley viscosity function may be derived from Eq. (2) and the concept of apparent viscosity of a generalized Newtonian liquid (GNL), $\eta(\dot{\gamma}) = \tau / \dot{\gamma}$, (Bird *et al.*, 1987) as follows,

$$\begin{aligned} \eta(\dot{\gamma}) &= \frac{\tau_0}{\dot{\gamma}} + K \dot{\gamma}^{n-1} & \text{if } \tau > \tau_0 \\ \dot{\gamma} &= 0 & \text{if } \tau < \tau_0 \end{aligned} \quad (5)$$

However, the classical Herschel-Bulkley model may find some drawback to describe a real viscoplastic material due to the discontinuity experienced by the shear stress. In virtue of this limitation, Papanastasiou (1987) proposed a regularization of Eq. (2) introducing a numerical parameter m that controls the exponential growth of the shear stress,

$$\tau = \tau_0 [1 - \exp(-m \dot{\gamma})] + K \dot{\gamma}^n \quad (6)$$

where the parameter m has time dimension. Nonetheless, even being of a straightforward computational implementation, the regularized model defined by Eq. (6) may not describe a well defined yield surface ($\tau = \tau_0$). From this equation, the material unyielded regions are no more rigid body but fluid zones subjected to finite high viscosities

Again, the regularized Herschel-Bulkley viscosity function may be achieved from the GNL apparent viscosity and Eq. (6), as follows

$$\eta(\dot{\gamma}) = \frac{\tau_0}{\dot{\gamma}} [1 - \exp(-m \dot{\gamma})] + K \dot{\gamma}^{n-1} \quad (7)$$

3. FINITE ELEMENT APPROXIMATION

Starting from the differential system defined by Eq. (1), a multi-field boundary value problem for steady-state flows of regularized Herschel-Bulkley fluids (Eq. 7) may be stated as

$$\begin{aligned} \rho[\nabla \mathbf{u}] \mathbf{u} + \nabla p - \operatorname{div} \boldsymbol{\tau} &= \rho \mathbf{g} && \text{in } \Omega \\ \operatorname{div} \mathbf{u} &= 0 && \text{in } \Omega \\ \boldsymbol{\tau} - 2(\tau_0(2 \operatorname{tr} \mathbf{D}^2)^{-1/2}) [1 - \exp(-m(2 \operatorname{tr} \mathbf{D}^2)^{1/2})] + K(2 \operatorname{tr} \mathbf{D}^2)^{(n-1)/2} \mathbf{D}(\mathbf{u}) &= 0 && \text{in } \Omega \\ \mathbf{u} &= \mathbf{u}_g && \text{on } \Gamma_g \\ -p \mathbf{I} + 2(\tau_0(2 \operatorname{tr} \mathbf{D}^2)^{-1/2}) [1 - \exp(-m(2 \operatorname{tr} \mathbf{D}^2)^{1/2})] + K(2 \operatorname{tr} \mathbf{D}^2)^{(n-1)/2} \mathbf{D}(\mathbf{u}) \mathbf{n} &= \mathbf{t}_h && \text{on } \Gamma_h \end{aligned} \quad (8)$$

where the variables ρ , p , \mathbf{u} , \mathbf{D} and \mathbf{g} , were defined as before, \mathbf{t}_h the surface force and the tensor $\boldsymbol{\tau}$ being decomposed as, $\boldsymbol{\tau} = \mathbf{T} + p \mathbf{I}$. (Astarita and Marrucci, 1974).

3.1. A multi-field stabilized formulation

The finite element approximation the multi-field problem defined by Eq. (8) were built employing the usual finite subspaces for velocity (\mathbf{V}^h), pressure (P^h) and stress ($\boldsymbol{\Sigma}^h$) fields,

$$\begin{aligned} P^h &= \{q \in C^0(\Omega) \cap L_0^2(\Omega) \mid p_{|K} \in R_m(K), K \in \Omega^h\} \\ \mathbf{V}^h &= \{\mathbf{v} \in H_0^1(\Omega)^N \mid \mathbf{v}_{|K} \in R_l(K)^N, K \in \Omega^h\} \\ \mathbf{V}_g^h &= \{\mathbf{v} \in H^1(\Omega)^N \mid \mathbf{v}_{|K} \in R_l(K)^N, K \in \Omega^h, \mathbf{v} = \mathbf{u}_g \text{ on } \Gamma^h\} \\ \boldsymbol{\Sigma}^h &= \{\mathbf{S} \in C^0(\Omega)^{N \times N} \cap L_2(\Omega)^{N \times N} \mid S_{ij} = S_{ji}, i, j = 1, N, \mathbf{S}_{|K} \in R_m(K)^{N \times N}, K \in \Omega^h\} \end{aligned} \quad (9)$$

where R_k, R_l denote, respectively, polynomial spaces of degree k and l (Ciarlet, 1978).

From finite element subspaces definitions introduced by Eq. (9), a multi-field stabilized formulation for Eq (8) may be written as follows: find $(\boldsymbol{\tau}^h, \mathbf{u}^h, p^h) \in \boldsymbol{\Sigma}^h \times \mathbf{V}_g^h \times P^h$, such that:

$$B(\boldsymbol{\tau}^h, \mathbf{u}^h, p^h; \mathbf{S}^h, \mathbf{v}^h, q^h) = F(\mathbf{S}^h, \mathbf{v}^h, q^h) \quad \forall (\mathbf{S}^h, \mathbf{v}^h, q^h) \in \boldsymbol{\Sigma}^h \times \mathbf{V}^h \times P^h \quad (10)$$

where

$$\begin{aligned} B(\boldsymbol{\tau}^h, p^h, \mathbf{u}^h; \mathbf{S}^h, q^h, \mathbf{v}^h) &= (2(\tau_0(2 \operatorname{tr} \mathbf{D}^2)^{-1/2}) [1 - \exp(-m(2 \operatorname{tr} \mathbf{D}^2)^{1/2})] + K(2 \operatorname{tr} \mathbf{D}^2)^{(n-1)/2})^{-1} \int_{\Omega} \boldsymbol{\tau}^h \cdot \mathbf{S}^h d\Omega \\ &- \int_{\Omega} \mathbf{D}(\mathbf{u}^h) \cdot \mathbf{S}^h d\Omega + \int_{\Omega} \rho[\nabla \mathbf{u}^h] \mathbf{u}^h \cdot \mathbf{v}^h d\Omega - \int_{\Omega} \boldsymbol{\tau} \cdot \mathbf{D}(\mathbf{v}^h) d\Omega - \int_{\Omega} p \operatorname{div} \mathbf{v}^h d\Omega + \int_{\Omega} \operatorname{div} \mathbf{u}^h q^h d\Omega + \epsilon \int_{\Omega} p^h q^h d\Omega \\ &+ \sum_{K \in \Omega^h} \int_{\Omega_K} (\rho[\nabla \mathbf{u}^h] \mathbf{u}^h + \nabla p^h - \operatorname{div} \boldsymbol{\tau}) \alpha(\operatorname{Re}_K) (\rho[\nabla \mathbf{v}^h] \mathbf{u}^h + \nabla q^h - \operatorname{div} \mathbf{S}^h) d\Omega + \delta \int_{\Omega} \operatorname{div} \mathbf{u}^h \operatorname{div} \mathbf{v}^h d\Omega \\ &+ (2(\tau_0(2 \operatorname{tr} \mathbf{D}^2)^{-1/2}) [1 - \exp(-m(2 \operatorname{tr} \mathbf{D}^2)^{1/2})] + K(2 \operatorname{tr} \mathbf{D}^2)^{(n-1)/2}) \beta \cdot \\ &\quad \cdot \int_{\Omega_K} ((2(\tau_0(2 \operatorname{tr} \mathbf{D}^2)^{-1/2}) [1 - \exp(-m(2 \operatorname{tr} \mathbf{D}^2)^{1/2})] + K(2 \operatorname{tr} \mathbf{D}^2)^{(n-1)/2})^{-1} \boldsymbol{\tau}^h - \mathbf{D}(\mathbf{u}^h)) \cdot \\ &\quad \cdot ((2(\tau_0(2 \operatorname{tr} \mathbf{D}^2)^{-1/2}) [1 - \exp(-m(2 \operatorname{tr} \mathbf{D}^2)^{1/2})] + K(2 \operatorname{tr} \mathbf{D}^2)^{(n-1)/2})^{-1} \mathbf{S}^h - \mathbf{D}(\mathbf{v}^h)) d\Omega \end{aligned} \quad (11)$$

and

$$F(\mathbf{S}^h, q^h, \mathbf{v}^h) = \int_{\Omega} \mathbf{f} \cdot \mathbf{v}^h d\Omega + \int_{\Gamma_h} \mathbf{t}_h \cdot \mathbf{v}^h d\Gamma + \sum_{K \in \Omega^h} \int_{\Omega_K} \mathbf{f} \cdot (\alpha(\operatorname{Re}_K) (\rho[\nabla \mathbf{v}^h] \mathbf{u}^h - \nabla q^h + \operatorname{div} \mathbf{S})) d\Omega \quad (12)$$

with $\varepsilon \ll 1$ and $0 \leq \beta \leq 1$, according Behr et al. (1993), and the stabilized parameters $\alpha(\text{Re}_K)$ and δ are given as in Franca and Frey (1992),

$$\begin{aligned} \alpha(\text{Re}_K) &= \frac{h_K}{r|\mathbf{u}|_p} \xi(\text{Re}_K) \\ \xi(\text{Re}_K) &= \begin{cases} \text{Re}_K, & 0 \leq \text{Re}_K < 1 \\ 1, & \text{Re}_K \geq 1 \end{cases} \\ \text{Re}_K &= \frac{\rho m_K |\mathbf{u}|_p h_K}{4(\tau_0(2 \text{tr} \mathbf{D}^2)^{-1/2} [1 - \exp(-m(2 \text{tr} \mathbf{D}^2)^{1/2})] + K(2 \text{tr} \mathbf{D}^2)^{(n-1)/2})} \\ m_K &= \min\{1/3, 2C_k\} \\ C_k &= \sum_{K \in \Omega^h} h_K^2 \|\text{div} \mathbf{S}^h\|_{0,K}^2 \geq \|\mathbf{S}^h\|_K^2 \quad \forall \mathbf{S}^h \in \Sigma^h \end{aligned} \quad (13)$$

in which $|\mathbf{u}|_p$ denoting the p -norm to \mathfrak{R}^N and the parameter m_k was derived from the error analysis established in Franca and Frey (1992).

Remark: Taking the stability parameter α equal to zero, the multi-field stabilized formulation defined by Eq. (10)-(13) recovers the classical Galerkin formulation for the boundary-value problem defined by Eq. (8). Besides, the usual expression of the grid Reynolds number was modified with the inclusion of the parameter m_k in Eq. (13), to take into account also the degree of interpolation used. (Franca and Frey, 1992).

3.2. Associated matrix problem

Substituting in Eq. (10)-(13) the finite element approximations for the trial solutions $(\boldsymbol{\tau}^h, \mathbf{u}^h, p^h)$ - and their respective test functions, namely $(\mathbf{S}^h, \mathbf{v}^h, q^h)$ - as a combination of their shape functions and unknown degrees of freedom, the following residual system of nonlinear equations may be achieved,

$$\mathbf{R}(\mathbf{U}) = \mathbf{0} \quad (14)$$

where \mathbf{U} is the vector of degrees of freedom at the nodal points, namely $\mathbf{U} = [\boldsymbol{\tau}, \mathbf{u}, \mathbf{p}]^T$, and the residual $\mathbf{R}(\mathbf{U})$ is given by

$$\begin{aligned} \mathbf{R}(\mathbf{U}) = & [(1+\beta)\mathbf{E}(\eta(\dot{\gamma})) + (1-\beta)\mathbf{H} + \mathbf{E}_\alpha(\mathbf{u})] \boldsymbol{\tau} + [\mathbf{N}(\mathbf{u}) + \mathbf{N}_\alpha(\mathbf{u}) - \beta\mathbf{K} - (1+\beta)\mathbf{H}^T - \mathbf{G}^T + \boldsymbol{\delta}] \mathbf{u} \\ & + [\mathbf{G} + \mathbf{G}_\alpha(\mathbf{u}) + \boldsymbol{\varepsilon}] \mathbf{p} - [\mathbf{F} + \mathbf{F}_\alpha(\mathbf{u})] \end{aligned} \quad (15)$$

where $[\mathbf{H}]$ is the matrix derived from the surface force term of motion, and $[\mathbf{H}^T]$ the matrix from the stress-deformation relation term of material equation, $[\mathbf{E}]$ the matrix from the extra-stress term of material equation, $[\mathbf{N}]$ the matrix from the inertia force term of motion equation, $[\mathbf{K}]$ the matrix from the diffusive term of material equation, $[\mathbf{G}]$ and $[\mathbf{G}^T]$ the matrices from the pressure term of motion equation and incompressibility term of continuity equation, respectively, $[\mathbf{F}]$ the vector from the body force-term of motion equation. Matrices subjected to α -subscript are derived from stabilized terms of motion equation, $[\boldsymbol{\delta}]$ the matrix from δ -stabilized-term of continuity and $[\boldsymbol{\varepsilon}]$ the matrix of the ε -term of continuity equation.

In order to solve the non-linear algebraic systems represented by Eq. (14)-(15), a quasi-Newton incremental method has been used. After an initial estimate for the degree of freedom vector has been set, $\mathbf{U}_{k=0}$, the following linear system must be solved at each Newton iteration,

$$\mathbf{J}(\mathbf{U}_k) \Delta \mathbf{U}_{k+1} = -\mathbf{R}(\mathbf{U}_k) \quad (16)$$

where the residual $\mathbf{R}(\mathbf{U})$ is given by Eq. (15) and the Jacobian matrix $\mathbf{J}(\mathbf{U})$ was defined by

$$\begin{aligned} \mathbf{J}(\mathbf{U}) = & (1+\beta)\mathbf{E}(\eta(\dot{\gamma})) + (1-\beta)\mathbf{H} + \mathbf{E}_\alpha(\mathbf{u}, \eta(\dot{\gamma})) + [\partial_{\mathbf{u}}(\mathbf{E}_\alpha(\mathbf{u}, \eta(\dot{\gamma})))] \boldsymbol{\tau} \\ & + \mathbf{M} + \mathbf{N}(\mathbf{u}) + \mathbf{N}_\alpha(\mathbf{u}, \eta(\dot{\gamma})) + \beta\mathbf{K} - (1+\beta)\mathbf{H}^T - \mathbf{G}^T + [\partial_{\mathbf{u}}(\mathbf{N}(\mathbf{u}) + \mathbf{N}_\alpha(\mathbf{u}, \eta(\dot{\gamma})))] \mathbf{u} \\ & + \mathbf{G} + \mathbf{G}_\alpha(\mathbf{u}, \eta(\dot{\gamma})) + \mathbf{P} + [\partial_{\mathbf{u}}(\mathbf{G}_\alpha(\mathbf{u}, \eta(\dot{\gamma})))] \mathbf{p} + \partial_{\mathbf{u}}(\mathbf{F}_\alpha(\mathbf{u}, \eta(\dot{\gamma}))) \end{aligned} \quad (17)$$

in order to obtain the incremental vector $\Delta \mathbf{U}_{k+1}$ and to update the degree of freedom vector,

$$\mathbf{U}_{k+1} = \mathbf{U}_k + \Delta \mathbf{U}_{k+1} \quad (18)$$

until the magnitude of the residual $\mathbf{R}(\mathbf{U}_k)$ be less than given tolerance value – in this paper, this value has been set as 10^{-7} .

Remark: Aiming to improve the convergence of the quasi-Newton algorithm, a continuation strategy acting on the advective matrices derived from the of motion equation has been implemented (Zinani and Frey, 2006). In addition, the algorithm has employed null velocity and pressure fields as initial estimates.

4. NUMERICAL RESULTS

In this section, multi-field stabilized approximations (Eq. (10)-(13)) for Herschel-Bulkley fluid flows, regularized by Papanastasiou strategy (Eq. (6) and (7)), through a sudden planar expansion have been carried out– see Fig. 1a for the problem statement. The channel aspect ratio has been defined by the relationship between the heights of the small and large channels, namely L_c/L_H , and was fixed as one-to-four. In order to guarantee fully-developed fluid flows in small and large channels, the following relationships have been set: $L_e/L_c=30$, for the small channel, and $L_s/L_c=45$, for the large one – with L_e and L_s standing for the lengths of small and large channels, respectively.

After a mesh independence test, over the error of the Euler pressure coefficient, a mesh employing 19,800 bi-linear Lagrangian finite element Q1/Q1/Q1 has been chosen – see Fig. 1b to a detail of the selected mesh at the expansion region.

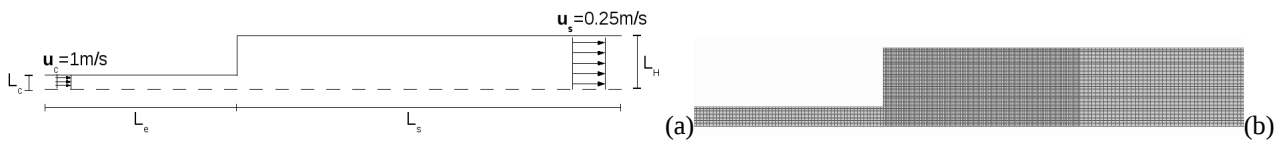


Figure 1. One-to-four sudden planar expansion flow: (a) Problem statement and (b) a detail of the selected mesh at the expansion region.

The imposed velocity and extra-stress boundary conditions were the following: in the channel inlet and outlet, a parallel uniform unity velocity profiles, preserving the flow mass conservation; no-slip and impermeability at channel walls; symmetry conditions at channel centerline, $\partial_{x_2} u_1 = u_2 = \tau_{12} = 0$, saving computational memory.

In order to evaluate the influence of the material yield stress and inertia on viscoplastic flow dynamics, the Herschel-Bulkley and Reynolds numbers have been introduced, respectively, as suggested in Alexandrou *et al.* (2001),

$$HB = \frac{\tau_0 L_c^n}{K u_c^n} \quad (19)$$

and

$$Re = \frac{\rho u_c^{2-n} L_c^n}{K} \quad (20)$$

with u_c and L_c standing for characteristic values of velocity and length, and the remaining variables were defined as previously.

In Fig. 2 τ -isobands were shown, aiming to investigate the yield stress limit on flow dynamics of a shear-thinning viscoplastic fluid. The flow has been supposed inertialess ($Re=0$), the Papanastasiou's regularizing parameter fixed as $m=10^3$, the power-law coefficient as $n=0.37$, and the Herschel-Bulkley number varying from $HB=0.1$ to 100. From the figure, the more the Herschel-Bulkley number increases, the more the unyielded material regions increase - black zones in the pictures – due to the material being subjected to higher values of shear stress limit, $\tau < \tau_0$. For $HB=0.1$ (Fig. 2a), the yielded regions - the white zones in the pictures - dominated the entire domain but a tiny unmoving unyielded region at expansion corner and a small plug flow around the channel centerline. For higher Herschel-Bulkley values, $HB=1-100$ (Fig. 2b-2d), this behavior was enhanced, with the unyielded region growth strongly dependent on the increasing of HB .

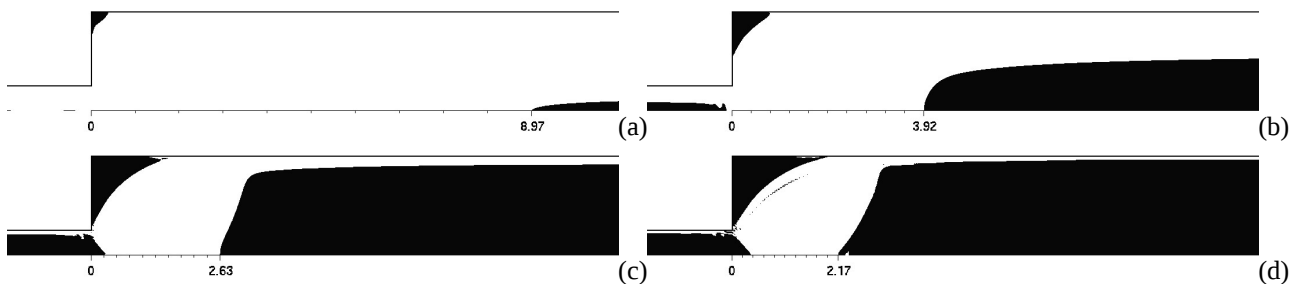


Figure 2. τ -isobands, for $n=0.37$, $m=10^3$ and $Re=0$: (a) $HB=0.1$, (b) $HB=1$, (c) $HB=20$, (d) $HB=100$.

In Fig. 3, the characterization of material unyielded regions has been also re-addressed introducing elevation plots for axial velocity, for the same parameter values investigated in Fig. 2 – $Re=0$, $m=10^3$, $n=0.37$ and HB from 0.1 up to 100. For all pictures, well-defined moving unyielded regions – or, simply, plug-flows – may be found around the centerline of the large channel, even for the lowest viscoplastic flow, $HB=0.1$ (Fig. 3a). For the two first flows in the small channel – for $HB=0.1$ (Fig. 3a) and $HB=1.0$ (Fig. 3b) - the transition from the inlet velocity profile to a thin plug-flow may be still observed, due to the high shear stresses experimented in the channel upstream the expansion ($\tau > \tau_0$). For higher values of HB , for $HB=20$ (Fig. 3c) and $HB=100$ (Fig. 3d), this development have disappeared with no visual transition to plug-flow profiles being verified.

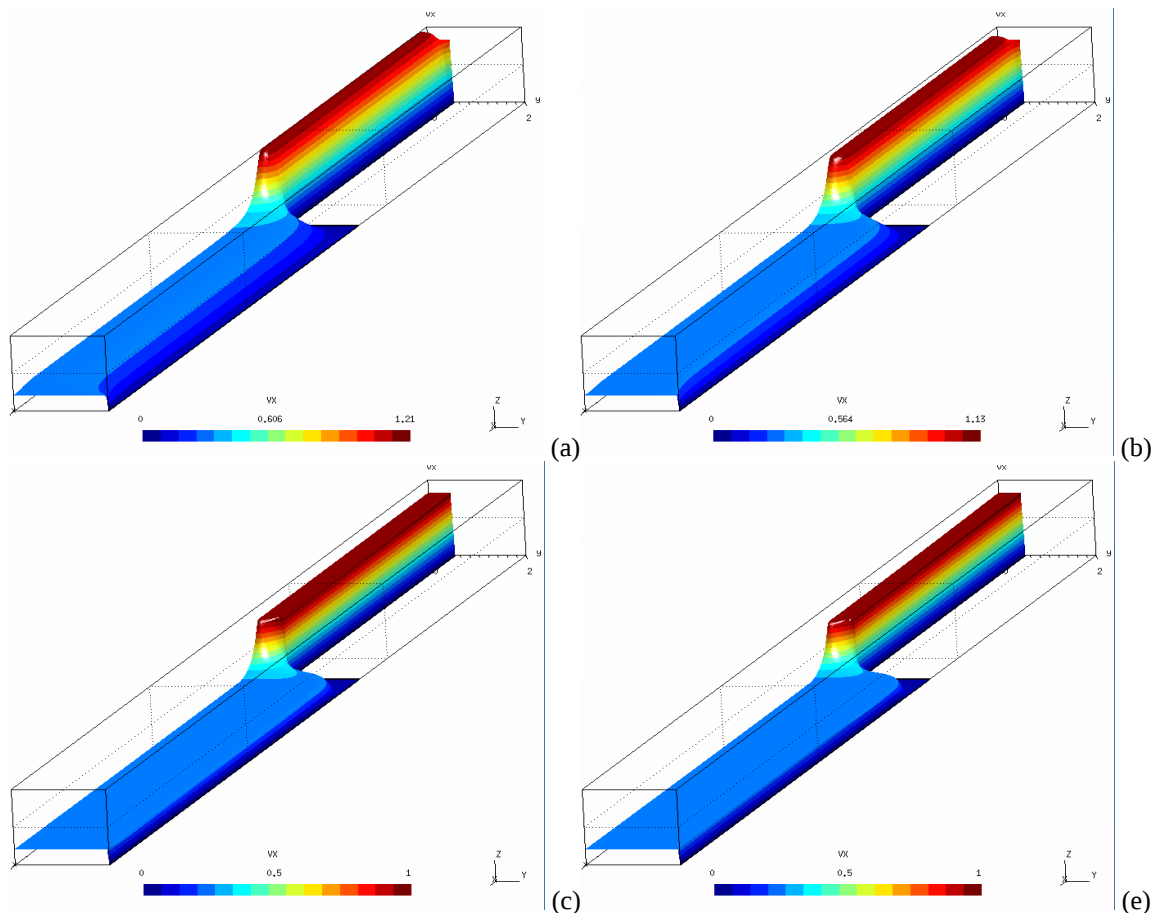


Figure 3. Axial velocity isobands, for $n=0.37$, $m=10^3$ and $Re=0$: (a) $HB=0.1$, (b) $HB=1$, (c) $HB=20$, (d) $HB=100$.

Fig. 4 has been introduced for two distinct reasons: from the mechanical point of view, to investigate the influence of the yield stress on the pressure drop through viscoplastic fluid flows; and, from the numerical point of view, to check the stability features of the stabilized method defined in Eq. (10)-(13). Again, creeping flow has been assumed and Herschel-Bulkley has been ranged from $HB=0.1-100$, for fixed values of $n=0.37$ and $m=10^3$. Firstly, from the pressure elevation plots shown in this figure, it may be observed that the pressure drop through the channel augmented with the HB increasing – as a result of the enlarging of unyielded regions which turned the flow much more viscous. Secondly,

all pictures in the figure have shown very stable pressure surfaces, attesting in this way the fine numerical stability of the employed stabilized method, even for very high Herschel-Bulkley fluid flows (HB=100 (Fig. 4d)).

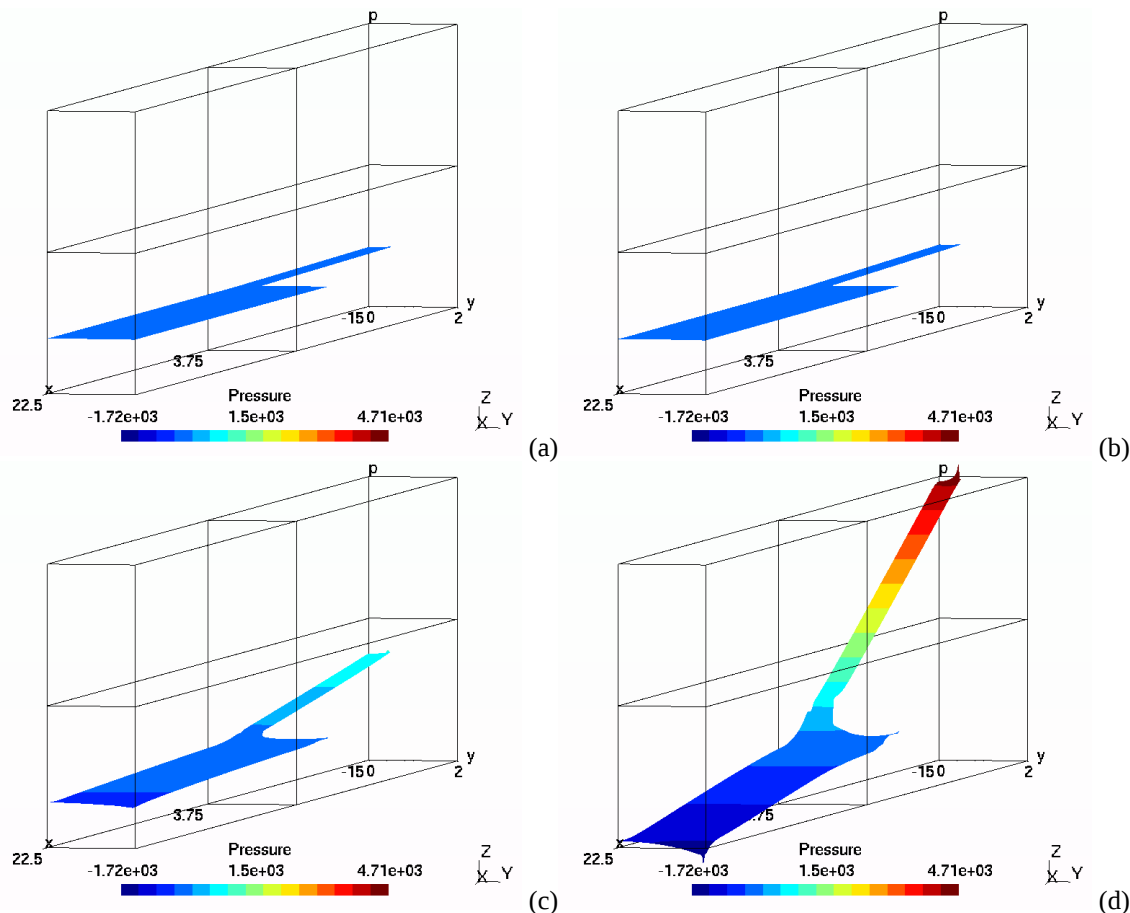


Figure 4. Pressure elevation plots, for $n=0.37$, $m=10^3$ and $Re=0$: (a) HB=0.1, (b) HB=1, (c) HB=20, (d) HB=100.

Now, comparing the pictures shown in Fig. 5 with the ones in Fig. 2, the influence of the power-law coefficient on the morphology of unyielded regions may be understood. In Fig. 5, τ -isobands have been depicted for a shear-thickening viscoplastic fluid, namely $n=1.5$, creeping flow ($Re=0$), $m=10^3$ and the same values of Herschel-Bulkley numbers presented in Fig. 2, *i. e.*, HB=0.1-100 (Fig. 2a-2d). The same dependence of the unyielded region morphology on HB increasing has been noticed, with the shear-thickening fluid presenting larger regions than the analogous regions of the shear-thinning viscoplastic fluid depicted in Fig. 2. This feature may be clearly observed comparing Fig. 2a-2b to Fig. 5a-5b, for the same values of HB=0.1 and HB=1.0, respectively.

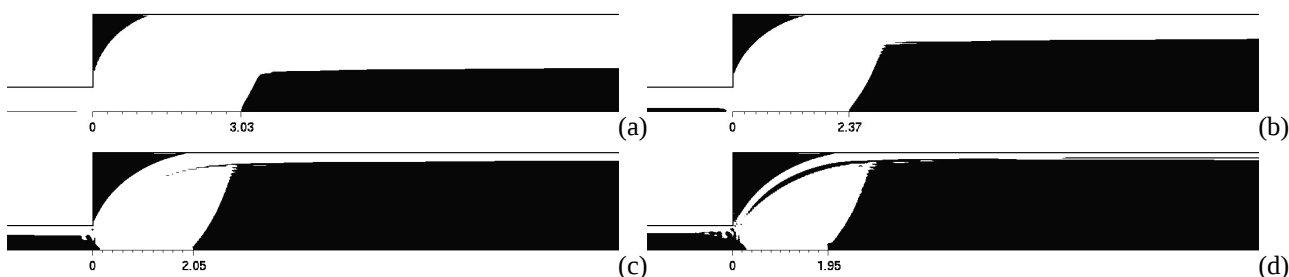


Figure 5. τ -isobands, for $n=1.5$, $m=10^3$ and $Re=0$: (a) HB=0.1, (b) HB=1, (c) HB=20, (d) HB=100.

In Fig. 6, the influence of the flow-rate on the growth of unyielded material regions has been investigated. In doing so, the flow was still supposed to be without inertia effects, for fixed values of HB=20, $n=0.37$ and $m=10^3$, and the dimensionless inlet axial velocity, $u^*=u/u_c$, varying from 2 to 20. As it has been illustrated by τ -isobands of these pictures, the more the flow-rate increased, the more the unyielded regions of the material decreased. This viscoplastic

behavior could be anticipated in virtue of the increasing flow-rate leading to higher shear rates and, according to power-law constitutive equation (Bird *et al.*, 1987), to higher shear stresses acting on the material along the channel ($\tau > \tau_0$).

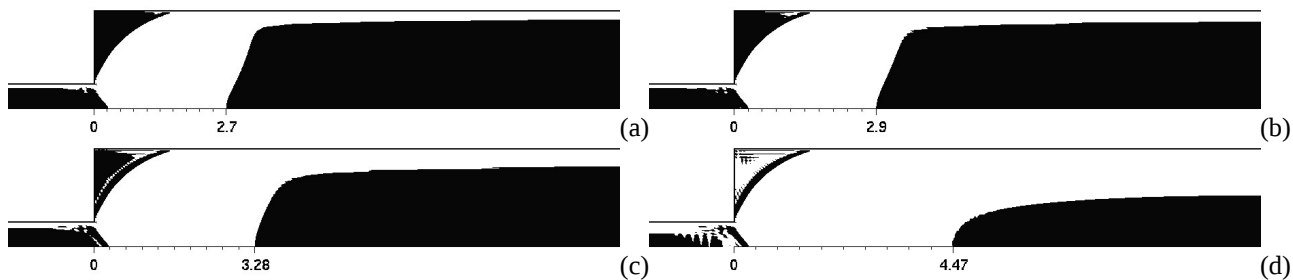


Figure 6. τ -isobands, for $HB=20$, $n=0.37$, $m=10^3$ and $Re=0$: (a) $u^*=2$, (b) $u^*=5$, (c) $u^*=10$, (d) $u^*=20$.

At last, the influence of inertia effects on the development of unyielded material regions has been presented in Fig. 7. Now, the flow has been no more assumed inertialess, with the Reynolds number simulated from 1 to 10, and the fluid rheological parameter set as $HB=20$, $n=0.37$ and $m=10^3$. The τ -isobands at expansion corner illustrated in the figure, suggest two distinct viscoplastic behaviors as Reynolds number increases. First, the unmoving unyielded regions at expansion corner showed a monotonic increasing for Reynolds values up to seven (Fig.7a-7c). Further, for higher values of Reynolds number, this region began to break up – with the applied shear stresses at expansion corner being higher than the material yield limit ($\tau > \tau_0$), due to inertia augmentation. Besides, the expansion vortex had its development constrained by the split unmoving unyielded regions (Fig.7d), originating in this way smaller vortex lengths than those experimented by a Newtonian fluid.

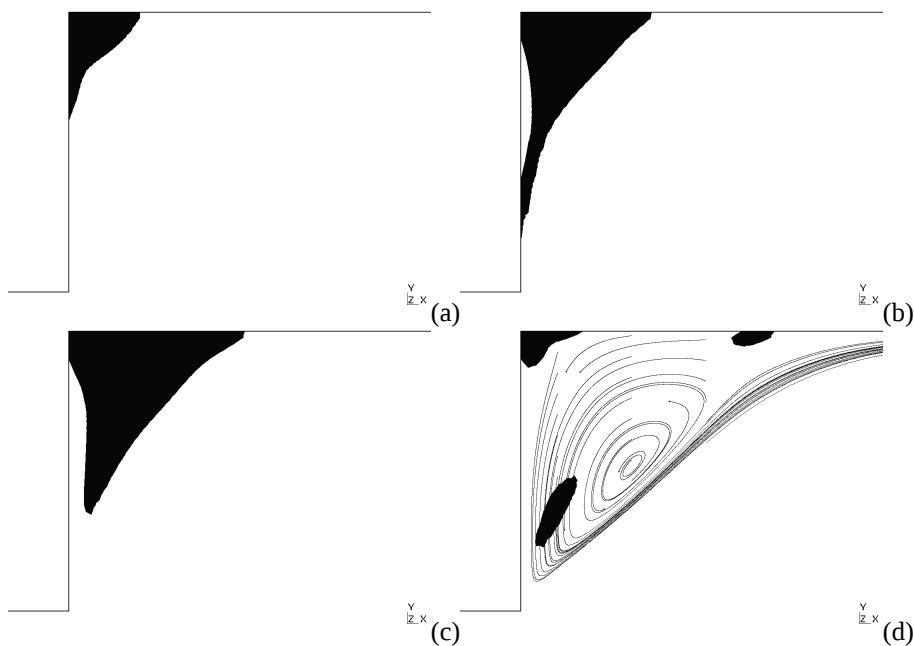


Figure 7. τ -isobands, for $HB=0.1$, $n=0.37$ and $m=10^3$: (a) $Re=1$, (b) $Re=5$, (c) $Re=7$, (d) $Re=10$.

5. FINAL REMARKS

In this article, finite element approximations for regularized Herschel-Bulkley fluids through an one-to-four sudden planar expansion have been undertaken. The employed mechanical model consisted of mass and momentum balance equations coupled with the Herschel-Bulkley viscoplastic equation, regularized by the equation introduced by Papanastasiou (1987). This model have been approximated by a multi-field stabilized method in extra-stress, velocity and pressure. In the numerical simulations, the Herschel-Bulkley number, the power-law index, the dimensionless inlet velocity and Reynolds number have been varied in order to investigate the influence of the material shear limit, the shear-thinning effect, the flow-rate and inertia on the morphology of the moving and unmoving unyielded regions of a viscoplastic material. For creeping flows, the more Herschel-Bulkley and the power-law index increased, the more

unyielded regions increased too. On the contrary, the more flow-rate increased, the more the unyielded regions decreased. At last, for inertia flows, the increasing of the Reynolds number continuously increased the unyielded regions at expansion corner, up to a critical value of the Reynolds number; beyond this value, the unyielded regions detached from expansion corner and began to break up. In all computations a combination of equal-order bi-linear Lagrangian interpolations for extra-stress, velocity and pressure, violating in this way the involved inf-sup conditions.

6. ACKNOWLEDGEMENTS

The author C. Fonseca thanks for its graduate scholarship provided by CAPES/REUNI and the author S. Frey acknowledges CNPq for financial support..

7. REFERENCES

- Alexandrou, A.N., McGilvrey, T.M., and Burgos, G., 2001, "Steady Herschel-Bulkley fluid in tree-dimensional expansions", *Journal of Non-Newtonian Fluid Mechanics*, Vol. 100, pp. 77-96.
- Astarita G., Marrucci G., 1974, "Principles of Non-Newtonian Fluid Mechanics" McGraw-Hill, London.
- Barnes, H.A., 1999, "The Yield stress – a review or 'παντα' – everything flows?", *Journal of Non-Newtonian Fluid Mechanics*, Vol. 81, pp. 133-178.
- Behr, A.M., Franca, L.P. And Tezduyar, T. E., 1993, "Stabilized finite element methods for the velocity – pressure – stress formulation of incompressible flows", *Computer Methods in Applied Mechanics and Engineering*, Vol. 104, pp. 31-48.
- Bird, R. B., Armstrong, R. C. and Hassager, O., 1987, "Dynamics of Polymeric Liquids". Vol.1, John Wiley & Sons, U.S.A.
- Brooks, A.N. and Hughes, T.J.R., 1982, "Streamline Upwind/Petrov-Galerkin Formulations for Convective Dominated Flows with Particular Emphasis on the Incompressible Navier-Stokes Equations", *Computer Methods in Applied Mechanics and Engineering*, Vol. 32, pp. 199-259.
- Ciarlet,P.G., 1978, "The Finite Element Method for Elliptic Problems". North Holland, Amsterdam.
- Franca, L.P., and Frey, S., 1992, "Stabilized finite element methods: II. The incompressible Navier-Stokes equations", *Comput. Methods Appl. Mech. Engrg.*, Vol. 99, pp. 209-233.
- Papanastasiou, T.C., 1987, "Flows of Materials with Yield", *Journal of Rheology*, Vol. 31, No. 5, pp. 385-404.
- Pascal, J., Magnin, A., and Piau, J.M., 2001. "Viscoplastic Fluid Flow Through a Sudden Axisymmetric Expansion ", *AIChE Journal*, Vol. 47, pp. 2155-2166.
- Zinani, F.; Frey, S., 2006, "Galerkin Least-Squares Finite Element Approximations for Isochoric Flows of Viscoplastic Liquids". *Journal of Fluids Engineering - Transactions of the ASME, USA*, Vol. 128, No.. 4, pp. 856-863.

8. RESPONSIBILITY NOTICE

The authors are the only responsible for the printed material included in this paper.